

Studying flowers in 3D using photogrammetry

Marion Leménager^{1,*}, Jérôme Burkiewicz¹, Daniel Schoen², and Simon Joly^{1,3}

¹*Institut de recherche en biologie végétale, Département de sciences biologiques, Université de Montréal, 4101 Rue Sherbrooke E, Montréal, QC H1X 2B2, Canada*

²*Biology department, McGill University, 205 Av. du Docteur-Penfield, Montréal, QC H3A 1B1, Canada*

³*Jardin Botanique de Montréal, 4101 Rue Sherbrooke E, Montréal, QC H1X 2B2, Canada*

*Corresponding author, marion.lemenager@umontreal.ca

October 26, 2022

ORCID ID

Marion Leménager 0000-0002-9936-9160
Jérôme Burkiewicz 0000-0001-6968-3506
Daniel Schoen 0000-0001-6066-3760
Simon Joly 0000-0002-0865-8267

Twitter

Marion Leménager @MarionLemenager
Jérôme Burkiewicz @J_Burkiewicz
Simon Joly @simjoly

Abstract

- Flowers are intricate and integrated three-dimensional structures predominantly studied in 2D due to the difficulty in quantitatively characterising their morphology in 3D. Given the recent development of analytical methods for high-dimensional data, the reconstruction of flower models in three dimensions represents the limiting factor to studying flowers in 3D.
- We developed a floral photogrammetry protocol to reconstruct 3D models of flowers based on images taken with a digital single-lens reflex camera, a turntable and a portable lightbox.
- We demonstrate that photogrammetry allows a rapid and accurate reconstruction of 3D models of flowers from 2D images. It can reconstruct all visible parts of flowers and has the advantage of keeping colour information. We illustrated its use by studying the shape and colour of 18 Gesneriaceae species.
- Photogrammetry is an affordable alternative to micro-computed tomography (microCT) that requires minimal investment and equipment, allowing it to be used directly in the field. It has the potential to stimulate research on the evolution and ecology of flowers by providing a simple way to access three-dimensional morphological data from a variety of flower types.

Keywords— Comparative morphology, Flower colour, Floral shape, Geometric morphometrics, Ultra close-range photogrammetry, Three-dimensional flower models

1 Introduction

2 Flower shape, size and colour influence the attraction of pollinators, the way pollinators access floral rewards, and
3 contingently the exchange of pollen between anthers and stigmas (Faegri and Van Der Pijl, 1979; Fenster et al., 2004;
4 Willmer, 2011). Flower shape is also important in wind-pollinated species (anemophily) as it influences interactions
5 with air flows and so determines efficient pollen release, dispersal and capture (Timerman and Barrett, 2019). Because
6 flowers are three-dimensional structures that interact with a three-dimensional biotic and abiotic environment for
7 conspecific exchange of pollen, characterising flower shape and colour in 3D is important to promote a comprehensive
8 understanding of flower development and the role of flower shape in the ecology and evolution of species.

9 Only recently has it become feasible to study the variation of flower shape in three dimensions (3D) due to the
10 development of methods to build 3D flower models. The first reconstruction of flowers in 3D used micro-computed
11 tomography (microCT, or HRCT for high-resolution CT) to acquire and visually render digital three-dimensional
12 shape data of both surfaces and internal structures (Stuppy et al., 2003). MicroCT helps to visualise minute plant
13 structures and to study their external 3D morphology and internal structures qualitatively and quantitatively. The
14 characterisation and comparison of these 3D flower models using geometric morphometrics (Rohlf and Marcus, 1993)
15 has opened a vast array of possibilities for the study of flowers in 3D, which was deemed to represent a “revolution”
16 for the study of flowers (van der Niet et al., 2010). Though other 3D modelling techniques are available such as
17 laser-scanning and structured light that record surfaces, microCT scanning remains the most common 3D digitization
18 technique applied to plant specimens (Mathys et al., 2013; Davies et al., 2017).

19 Despite the fact that several studies recently used 3D flowers models (Gamisch et al., 2013; Wang et al., 2015;
20 Dellinger et al., 2019; Hsu et al., 2020; Reich et al., 2020; Artuso et al., 2021, 2022), the widespread analysis of 3D
21 flowers has not occurred. Geometric morphometrics studies of flowers in 3D are still limited compared to the mass of
22 literature in the fields of anthropology, zoology and paleontology. This could be due in part to the difficulties of using
23 microCT on the soft tissues of flowers, even though solutions for optimising HRCT scanning of flowers have been
24 proposed (e.g., Staedler et al., 2013; Dellinger et al., 2019). In addition, and perhaps more importantly, the high cost
25 of microCT techniques (Mathys et al., 2013) contributes to reducing their accessibility. Lastly, the fact that flower
26 colour is lost when reconstructing 3D models using X-ray scanning technologies (Mathys et al., 2013) limits the use
27 of this technique for studies interested in colour or colour patterns.

28 Recently, research based on 3D imagery has evolved rapidly and has received considerable attention (e.g., Katz and
29 Friess, 2014; Cunliffe et al., 2016; Evin et al., 2016; Ströbel et al., 2018; Christiansen et al., 2019; Giacomini et al., 2019;
30 Florey and Moore, 2019; Iglhaut et al., 2019; Medina et al., 2020). A 3D technique of interest is photogrammetry (or
31 structure from motion), which uses a collection of digital images to reconstruct a 3D model (see Linder, 2009; Luhmann
32 et al., 2013). Photogrammetry was originally used to reconstruct models of landscapes, buildings or large objects, but
33 it can also be used for medium (close-range photogrammetry) or small objects (ultra-close-range photogrammetry).
34 In short, photogrammetry begins by taking pictures of an object from all angles, ensuring that all aspects of the
35 object are present in several overlapping photos. The sets of photos are then aligned using the relative position of
36 homologous points in the overlapping pictures in a 3D space, and picture information is then used to reconstruct a 3D
37 model with colour (see *Floral photogrammetry protocol* and Fig. 1 for more detailed information). Although used in
38 many fields of biological sciences, photogrammetry has not yet been applied to the study of flowers.

39 The objective of this study is to demonstrate the potential of photogrammetry to reconstruct 3D models of flowers
40 to facilitate studies of floral shape and colour. We describe an affordable and portable photogrammetric setup that
41 could be used in the field, and outline a detailed protocol for reconstructing 3D photographic models of flowers of
42 various shapes, colours and sizes. To illustrate the approach, we present an example of application in the study of the
shape and colour of flowers from species of the Gesneriaceae.

44 2 Floral photogrammetry protocol

Here, we provide a summary of the photogrammetry protocol we developed. The full protocol is available from Github
46 (<https://github.com/plantevolution/photogrammetry-protocol>) and details of the source and costs of materials,
tools and software are provided as Supporting Information (Table S1). Specific terms in photography, 3D modelling
48 and geometric morphometrics are defined in the glossary (Box 1). Our objective is not to provide a unique and final
50 protocol, but to provide guidelines for users to employ photogrammetry to 3D model flowers and guide them on how
to adapt this approach for their own system.

52 2.1 Image acquisition

52 The first step of photogrammetry involves acquiring photos encapsulating flower details for later modelling in 3D. This
step is perhaps the most important as high quality images are key to produce high quality 3D models. We capture
54 images using a digital single-lens reflex (DSLR) camera and a fixed focal-length macro lens. We save images in RAW
format using an aperture of F16 (highest field depth without deteriorating the image quality), lowest ISO (e.g. 100)
56 to avoid image noise created by the sensor, and a shutter speed adjusted to allow the appropriate amount of light to
reach the camera's sensor to result in a well-exposed image (see Supporting Information Table S2 for a summary of
58 the settings we used).

To facilitate the photo capture of the flower from all directions, we use a turntable and automated remote camera
60 control (Fig. 1a,b). To help later photo processing and mask the background in the pictures, we recommend using
a uniform background. Good lighting conditions are also necessary for optimal picture quality. These conditions can
62 be recreated in the field using a portable lightbox (see Supporting Information Table S1).

The flower to be photographed is fixed at the centre of the turntable using pins or clamps, or could be placed in a
64 tube or a cut pipette tip depending on the structure and stiffness of the flower (see example Fig. 1c). A scale should
be placed so that it is visible in several photographs to allow scaling of the resulting model.

66 To capture the entire flower surface and details, we take a 360° series of photos of flowers placed in normal and
inverted positions (e.g., ventrally and dorsally). Typically 20 photos per rotation were taken at 3 different camera
68 heights and angles of approximately 0°, 30° and 60° for each side of a flower (see Fig.1b), for a total of 120 photos
per flower. Depending on the flower complexity, the number of photos, camera angles and flower positions can be
70 adjusted to capture all visible floral details. It is also possible to add close-ups photos to enhance the model and
reveal concealed and minute parts (e.g., reproductive organs). If using a variable focal lens, it is preferable that the
72 focal length is kept identical for all the pictures, and ideally at the minimum or maximum focal length possible to
avoid optical deformations (Agisoft LLC, 2021).

74 2.2 Colour and exposure calibration

Photographs must be colour-calibrated to adjust the reflectance and colour of an object and allow accurate comparison
76 between flowers (Troscianko and Stevens, 2015). To calibrate multiple photos with the same parameters, we use DNG
(Digital Negative) colour profiles created from an additional RAW photo of a standardised colour chart, taken for
78 each series of photos of a flower under the same light conditions and camera parameters. We convert the colour chart
in a DNG profile (e.g. using Adobe Digital Negative converter) and standardise the series of photos corresponding
80 to the colour chart (using e.g. Adobe Lightroom (Adobe Inc., San Jose, California, USA)), providing an accurate
reproduction of the flower colour for subsequent analyses of pigmentation patterns. We also standardise the photo
82 exposure using a 75% grey colour chip from the colour chart. Exposure calibration can also be performed at a later
stage directly using the colour file (texture) of the 3D model. From the calibrated RAW photos, we export JPG
84 images for the model reconstruction (Fig. 1c,d,e).

2.3 3D model reconstruction

86 The procedure we use to obtain a 3D model from photogrammetry includes photo alignment, which results in a sparse
87 three-dimensional point cloud, surface generation through depth maps calculation, and texture generation using the
88 projection of photos onto the surface of the model. Our protocol uses the commercial software Agisoft Metashape
89 Professional Edition version 1.7 (Agisoft LLC., St. Petersburg, Russia), but open-source photogrammetry software
90 also exist (see Medina et al. (2020) for more details).

91 During photo alignment (also referred as camera alignment), source images are positioned by searching for common
92 points in the photos (tie points) and by using the triangulation of the matching points. The alignment procedure can
93 customarily be done in a single step, by attributing images from different flower positions to distinct camera groups,
94 or by separating images from different flower positions into different chunks. Treating sets of images separately can
95 be useful for merging models of different flower parts (e.g. for modelling a complete flower by merging the flower with
96 and without its perianth). Chunks of images can also be treated separately during the alignment procedure when
97 the overlap between pairs of images isn't optimal to facilitate the alignment calculation (Fig. 1f,g,h,i, showing an
98 example with two chunks of images). Prior to aligning images, masks can be captured manually or automatically
99 to separate the flower from the background and restrict the searching of common points between images during the
100 alignment procedure to the flower itself (Fig. 1g). The picture alignment (Fig. 1h) generates a three dimensional
101 cloud of matching tie points for each set of images (Fig. 1i). When different chunks of images are used separately, they
102 need to be aligned together and then merged either automatically or by using manually-placed markers on distinctive
103 features on the flowers on several images (e.g. tips of petals or sepals, anthers). If manual markers are used, a
104 minimum of 3 markers spaced on the flower is required. The merging of images or groups of images results in a single
105 tie point cloud (Fig. 1j).

106 Once all the images are aligned around a single tie point cloud, the model (mesh) can be generated, using depth
107 maps generated for each photo that represent the distance of the flower surface on the z axis for each camera positions
108 (Fig. 1k). The mesh is composed of vertices, edges and faces, together forming polygons (Fig. 1l). During mesh
109 reconstruction, the interpolated colour of the mesh polygons is calculated from images when using depth maps as
110 source information (Fig. 1m). The resulting mesh may need minor touch-ups, such as removing unwanted portions
111 of the inflorescence or the pin used to attach the flower.

112 We then scale the model by manually positioning landmarks on the scale bar in the original images and defining
113 these landmarks as being spaced by the length of the scale, which resizes the model accordingly. Finally we build the
114 texture (detailed colour) of the model by using the 2D picture's information to generate a realistic visualisation of
115 the flower surface in 3D (Fig. 1n,o). The flower surface mesh can subsequently be used in geometric morphometric
116 applications (Fig. 1p,q) and the three-dimensional textured surface can be exported as a 2D layout of the 3D surface,
117 used in quantification of flower colour using each pixel colour information (Fig. 1r,s).

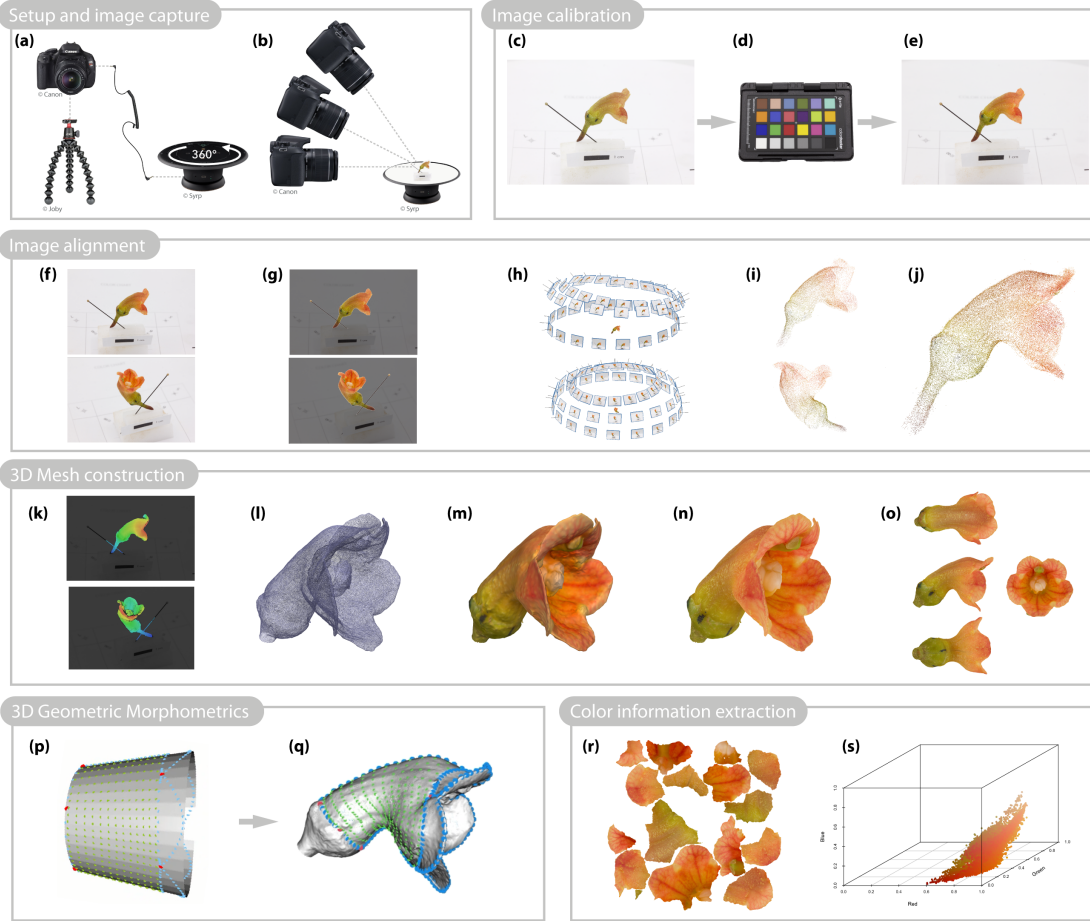


Figure 1: Graphical workflow of the photogrammetric approach used to study floral morphology and colour in three dimensions (3D). Flowers are attached to a 360°turntable that automatically triggers a camera as the turntable rotates in steps of a few degrees and are photographed using three camera angles for both ventral and dorsal view (a-b). All RAW images (c) are calibrated identically using a colour chart (d) to obtain realistic colour representation of flowers (e). Masks are applied to remove the background (f-g) before aligning the images (h), which results in a tie point cloud of homologous pixels detected in multiple photos (i). The separate sets of photos are then aligned and merged to give a unique tie points cloud (j). Using depth maps (k), a 3D mesh is reconstructed (l) and the interpolated colour of the mesh polygons is calculated from images (m). A more realistic 3D model is obtained by building the texture from the original photos (n), providing a finely detailed and coloured 3D model on the outer and inner surfaces of the flower (o). Landmarks (in red) and semi-landmarks are positioned on the flower model for curves (in blue) on the petal margin, petal base, dorsal and ventral corolla curvature, and the base of the sepals, as well as on the simplified truncated cone template. Surface semi-landmarks (in green) are automatically applied on flowers according to the template (p-q). The flower texture wrapping the model can be extracted as a 2D representation of the 3D surface (r) and used to analyse and quantify colour variation of the entire flower surface (s).

Box 1 - Glossary

Photography

Aperture: Size of the opening of a lens's diaphragm (or generically called shutter) through which light passes, noted f/N .

ISO: Camera sensor sensitivity to light.

Sensor: Part of the camera that detects and transforms light into information to produce an image.

Shutter speed: Time during which the shutter allows light to reach the sensor.

3D Modelling

3D Mesh (3D object): Structural tri-dimensional shape built of polygons along x,y and z axes to represent its height, width and depth.

Depth map: An image in which a colour gradient indicates the distance from the camera.

Edge: A connection between vertices.

Key point: A distinct feature recognised in a single image.

Mask: A delimited region of a photograph that is not the main subject.

Texture (or texture map): 2D object with details of the surface appearance, or information about the colours used to wrap a 3D object.

Tie points: Automatically detected or manually placed 3D points that are matched in multiple images and used to compute their 3D position.

Vertex: A position in a 3D space with three-dimensional x,y, and z coordinates.

Vertex colours: colours applied to each vertex according to the average colours of the corresponding areas on the images source.

Geometric morphometrics

Landmark: Fixed point at a particular position, usually on a distinguishable homologous feature.

Semi-landmark: Sliding point between landmarks or other semi-landmarks, describing curves or surfaces.

118

3 Performance of the photogrammetry approach

120 The above protocol was applied to diverse flowers selected to represent a variety of floral forms, colours and complexity. These were taken from species belonging to different Angiosperm families such as the Fabaceae (*Phaseolus coccineum*),
122 Cactaceae (*Schlumbergera sp.*), Lamiaceae (*Salvia nemorosa*), as well as 19 Gesneriaceae species from the living collections of the Montreal Botanical Garden, mainly from the genera *Rhytidophyllum* and *Gesneria* (see example
124 below for more information on these specimens). Flowers from 5 species modelled by photogrammetry were also scanned using microCT to compare models originating from both approaches.

126 3.1 3D flower reconstruction

The overall 3D reconstruction process using photogrammetry took from 0.5 to 2h depending on the complexity
128 of the project and the computer resources. The 3D models, the RAW photogrammetry image series to generate these models, and the corresponding colour charts and calibrated textures can be accessed from MorphoSource
130 (<https://www.morphosource.org/>) under the project "Gesneriaceae of the Montreal Botanical Garden".

The photogrammetric approach generated models of high quality that accurately represent the shape and colour
132 of flowers of different structures, sizes (2cm to 8cm), and symmetry (see Fig. 2 for a sample of flower models). The flower models presented in figure 2 were also deposited in SketchFab (sketchfab.com/plantevolution), an online
134 platform for hosting and visualising 3D models with textures, to allow a closer inspection of the models. In many cases, very minute details could be modelled, such as the delicate petal margins of *Rhytidophyllum vernicosum* (Fig.

¹³⁶ **2g)** or the styles and stamens of several species (Fig. **2c, d, e, f**). Overall, the flower shape and colour of the models were very accurate and were essentially identical to the real flowers.

¹³⁸ Some structures are more difficult to reconstruct, particularly those that are slender, translucent or reflective. Pillose organs were also challenging, in part due to the difficulty of applying masks. Structures that are very close to each other such as overlapping petals (*Schlumbergera* sp.; Fig. **2b**) or styles that very close to petals (Fig. **2f, h, i**) were also difficult to reconstruct independently from each other. Finally, very thin surfaces or parts that were partly concealed depending on the camera angles may require more source images to be further improved such as below the basal petal surfaces on *Schlumbergera* sp., the petal margins inside the corolla on *Phaseolus coccineum*, and the dorsal midrib of the sepal on *Salvia nemorosa*. Despite the occurrence of slight imperfections in some of the models, the global shape and colour of flowers reconstructed should allow most downstream applications.

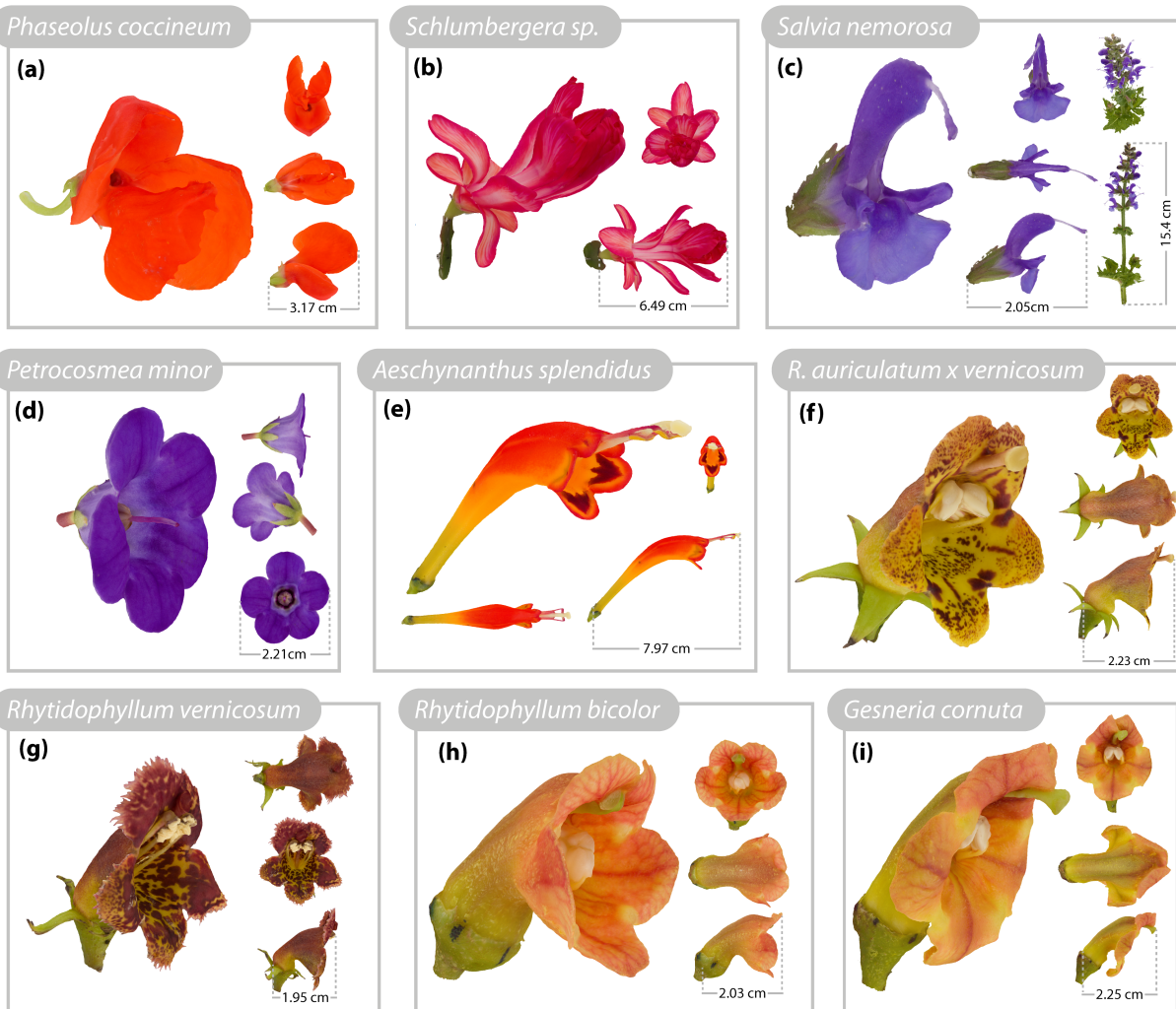


Figure 2: 3D textured models derived from non-Gesneriaceae (a-c) and Gesneriaceae flowers (d-i) using photogrammetry. *Phaseolus coccineum*, Fabaceae (a), *Schlumbergera* sp., Cactaceae (b), *Salvia nemorosa*, Lamiaceae (c). *Petrocosmea minor* (d), *Aeschynanthus splendidus* (e), the hybrid *Rhytidophyllum x vernicosum* (f), *Rhytidophyllum vernicosum* (g), *Rhytidophyllum bicolor* (h), and *Gesneria cornuta* (i), Gesneriaceae. The model of the inflorescence of *S. nemorosa* is illustrated under two different viewing angles (c).

¹⁴⁶ **3.2 Photogrammetry vs. microCT comparison**

To compare the models obtained by photogrammetry with models obtained by microCT scanning, the flowers of five species (*Gesneria acaulis* 1328-2021, *Kohleria sp.* 1828-2013, *Paliavana prasinata* 1432-2010, *Rhytidophyllum exsertum* 112-1991 and *Rhytidophyllum tomentosum* 1327-2021) were sent to the Integrated Quantitative Biology Initiative (IQBI) platform at McGill University for microCT scanning and model reconstruction. Flowers were collected at the Montreal Botanical Garden and fixed in 4% Paraformaldehyde (PFA) in 1X Phosphate-buffered saline (PBS). The samples were gradually transferred to 70% ethanol from water and placed in 2% ethanolic phosphotungstic acid (EPTA) in 70% ethanol stain for 15 days. Flowers were scanned in 1% agarose in 15 ml tubes at resolution 22 μ m at voltage 60V. The microCT models were reconstructed in Dragonfly (version 2020.2). The reconstruction of the models obtained from microCT took between 0.5 to 5h.

To allow a visual comparison of the models obtained by photogrammetry and microCT, we presented the flower models of three species side-by-side in different figures (Fig. 3 and Supporting Information Figs. S1 and S2). All microCT models were also analysed alongside the photogrammetry models in a geometric morphometric analysis (see application example below). The microCT models were deposited in Morphosource in the same project as the photogrammetry models.

The surface meshes of models reconstructed with the microCT scans included holes as well as bumps due to the detection of hairs during the scanning step, but overall represented the morphology of flowers similarly to photogrammetry (see details in the floral shape analysis application example). Due to the softening of tissues during the staining process, flower parts were occasionally distorted and flowers with naturally recurved petals and/or sepals during the anthesis were slightly unfolded on the CT-based model compared to the photogrammetry model and the real flower (see for instance *Paliavana prasinata* in Fig. 3a,b,c,d). Similar distortions of the corolla and sepals in microCT models are evident on the models of *G. rupinicola* and *R. exsertum* (Supporting Information Fig. S1, and S2). Internal and non-visible organs were properly modelled using microCT scan, which could not be accurately reproduced using photogrammetry (Fig. 3e,f). However, anther and stigma position can only be captured when visible from the flower opening (see Figs. 2 and 3).

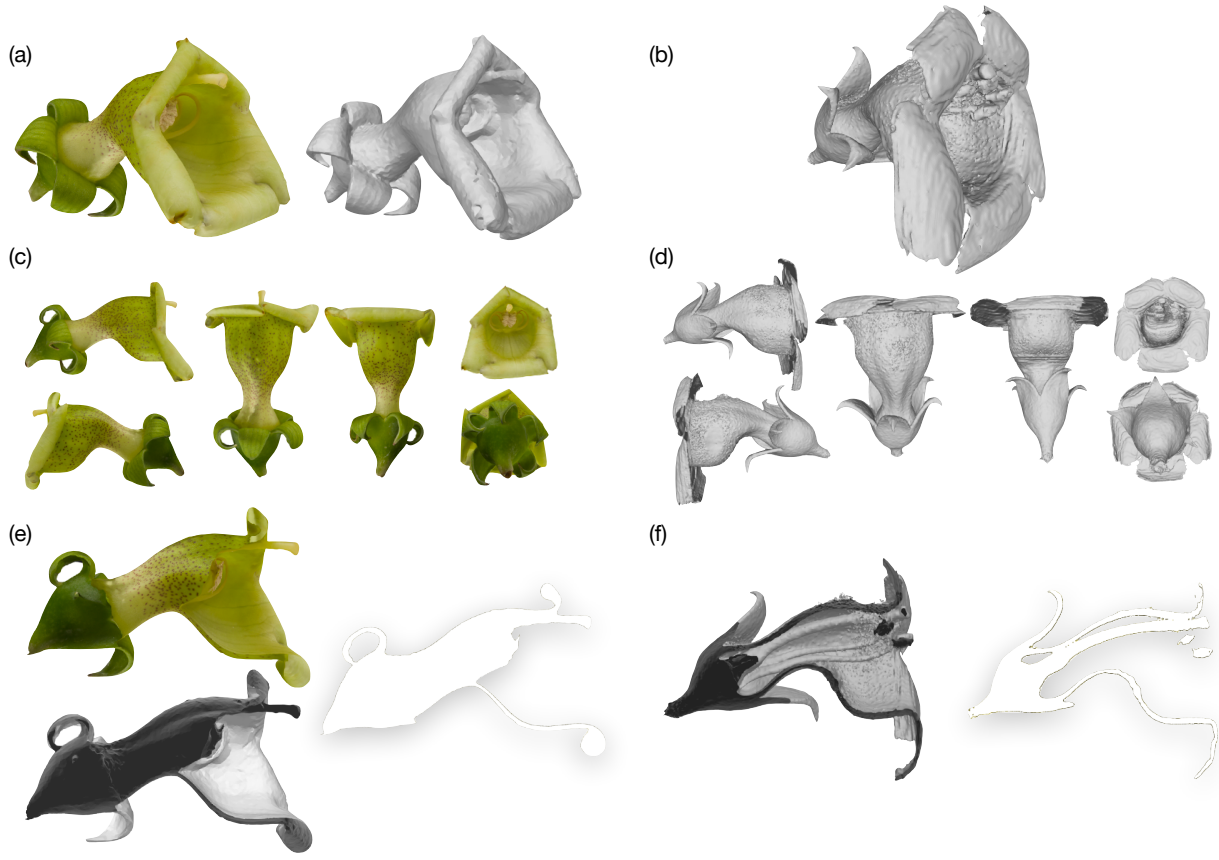


Figure 3: Comparison of 3D models of *Paliavana prasinata* derived from photogrammetry (left) and microCT (Micro Computed Tomography) scanning (right). The final solid models are represented for both photogrammetry (a - grey scale and colour) and microCT scan (b) under all viewing angles (c,d) (left and right lateral views, ventral, dorsal, anterior, and posterior views). Sections of these models are represented by half models (grey scale and colour) and median plane sections of both models along the x axis (e,f).

4 Application example

172 4.1 Material and methods

To demonstrate the potential use of flower models obtained from photogrammetry, we studied the shape and colour of
 174 26 flowers from 18 species and one hybrid (*Rhytidophyllum auriculatum* × *vernicosum*) from the Gesneriaceae family
 that belong to three pollination syndromes: bird pollination, bat pollination, and mixed-pollination (see details in
 176 Supporting Information Notes S1 and Table S3). We provide a brief description of the methods used here, but
 detailed materials and methods are available as supplementary information.

178 4.2 Floral shape analysis

The perianth of each flower was reconstructed in 3D using the described photogrammetry protocol above. We then
 180 used geometric morphometrics to compare the 3D flower shapes. Landmarks as well as semi-landmarks for curves and
 surfaces were placed on the flowers (see Supporting Information Methods S1, Fig. S3, and Table S4). After shape
 182 alignment using a generalized Procrustes analysis (GPA), the coordinates of the landmarks and semi-landmarks were

projected onto the tangent space using principal component analysis (PCA) (Supporting Information Methods S1).
 184 The resulting morphospace places individuals from the same species very close to each other and allows the distinction
 185 of the pollination syndromes (Fig. 4 and Supporting Information Fig. S4). The estimated mean 3D shape of each
 186 syndrome also shows the main differences in shape between them (Supporting Information Fig. S5). The inclusion of
 187 the microCT flower models to the same morphospace shows that they fall very close to the photogrammetry models
 188 (Supporting Information Fig. S6).

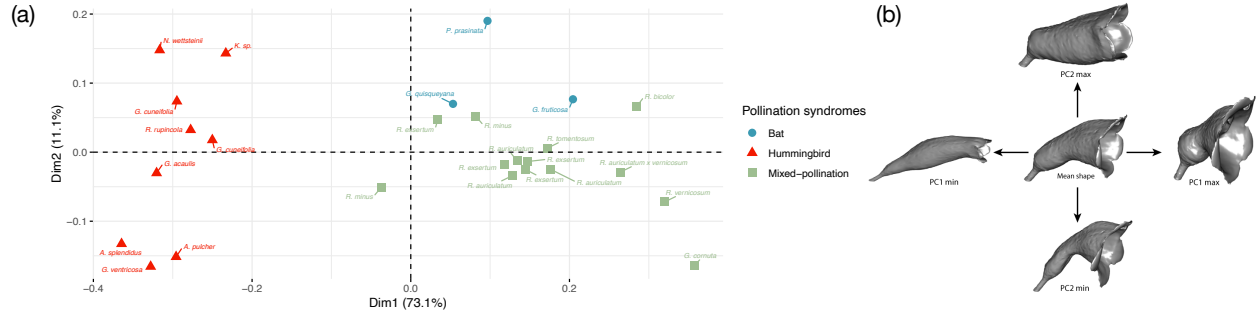


Figure 4: 3D floral morphospace and corresponding shape variation along the axes for individuals belonging to the *Gesneria*, *Rhytidophyllum*, *Nematanthus*, *Aeschynanthus*, *Kohleria*, and *Paliavana* genera. Specialists for bat (blue circles) and hummingbird pollination (red triangles) as well as mixed-pollination strategies (green squares) are represented along the first and second dimensions of the principal component analysis (PCA) (a). The mean 3D flower shape, as well as the maximum and minimum configurations of the 3D flower shape are shown for the first and second dimensions of the PCA (b).

4.3 Colour analysis

190 To illustrate the potential of the photogrammetric approach to study flower colour, the colour profiles of flowers were
 191 compared alongside the phylogeny of the 18 species of Gesneriaceae (see Supporting Information Methods S2 for
 192 phylogeny reconstruction). The colour of each flower surface texture was quantified in eight categories (bins) in terms
 193 of red, blue, and green, which then allowed to compute a colour distance between flowers (see Supporting Information
 194 Methods S3 and Fig. S7). The resulting distance matrix was used to build a phenogram and compared to the
 195 phylogenetic relationships (Fig. 5). This example highlights that species tend to group by pollination syndromes
 196 when considering flower colour and that similar colour patterns show evolutionary convergence in the Gesneriaceae.

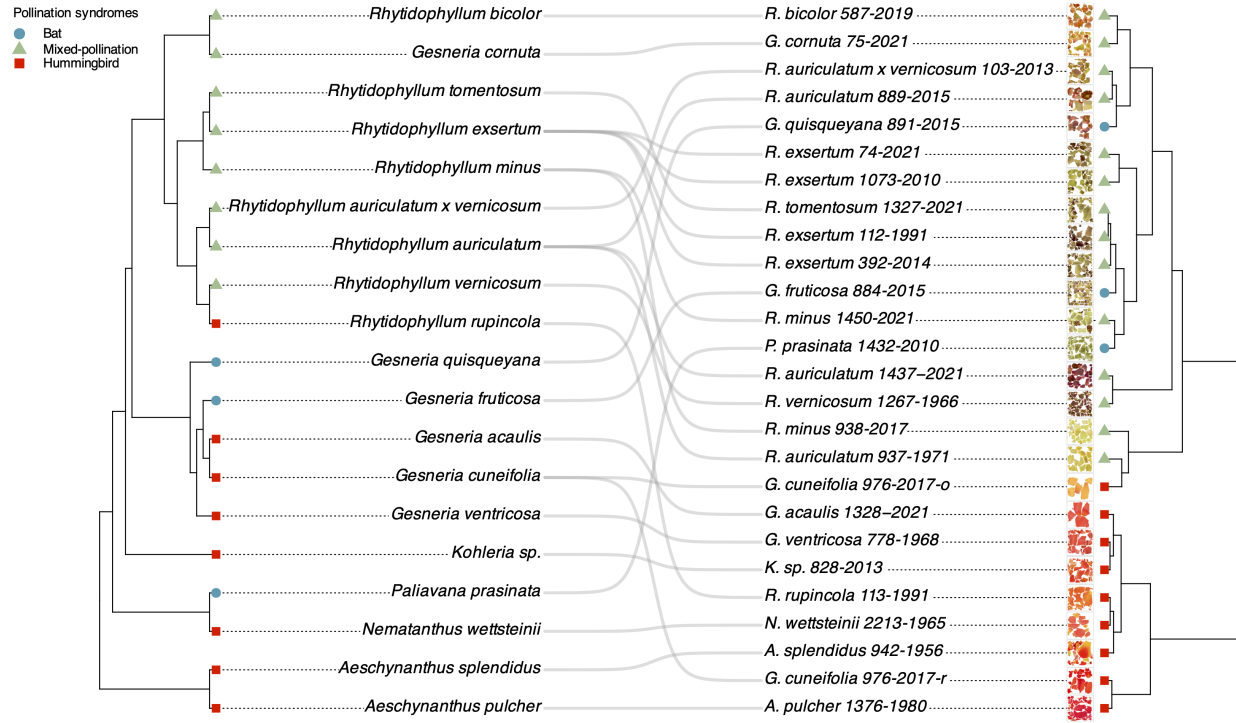


Figure 5: Tanglegram linking the phylogenetic relations of Gesneriaceae species (left) with the colour distance dendrogram from flower specimen colour using Ward's clustering method (right) according to their respective pollination syndromes.

5 Discussion

198 5.1 Relevance of ultra-close-range photogrammetry for the study of flowers

Flower shape has attracted much interest in several sub-fields of plant sciences, but relatively few studies have used
 200 3D flower models, despite the importance of precisely quantifying the size, shape and colour of flowers in 3D given that
 the vast majority of flowers have to interact in a three dimensional environment to be fertilised. The main aspects of
 202 the methods currently used that may limit the number of 3D geometric morphometric studies on floral shape are the
 cost and lack of portability of microCT technologies. Although flowers can be fixed in the field in highly concentrated
 204 ethanol for later microCT scanning, doing so can damage or shrink flowers depending on their structure and thickness
 (Staedler et al., 2013; Dellinger et al., 2019). Moreover, contrasting reagents used to infiltrate the flower tissues prior
 206 to scanning may also produce additional leaching artefacts (Staedler et al., 2013). We observed slight anatomical
 208 distortions in the flower models obtained with CT scans following fixation such as the unfolding of petals and sepals,
 distorting the shape and the relative positioning of the floral structures. Our microCT protocols could be improved
 210 to provide better and more accurate results; however, the use of standard protocols combined with an external service
 offers a fair comparison with our photogrammetry approach.

An array of flower sizes and colours for species belonging to the Gesneriaceae, Fabaceae, Lamiaceae, and Cactaceae
 212 were successfully reconstructed using photogrammetry. Various sizes of flowers as well as inflorescences can be rendered
 accurately and in detail and we were able to model all visible parts of the flowers, including the stigma and anthers
 214 in many species. The entire physical set-up (turntable, lightbox, tripod and colour chart) required to implement
 this method costs less than 600 US\$, making this approach affordable for most laboratories that already own a
 216 suitable digital camera. Computer requirements are relatively reasonable for photogrammetry applications (16-32 GB

of Random Access Memory (RAM), and 4-8 central processing units (CPUs)). The academic professional edition of
218 the Agisoft Metashape software we used to reconstruct the 3D models currently costs 549 US\$, although cheaper or open-source alternatives are available (see Medina et al. (2020)).

220 Ultra-close-range photogrammetry has several clear advantages over microCT—the gold standard in the field—for
reconstructing 3D models of flowers. It is portable, affordable, time efficient both for image acquisition and model
222 building, and can reconstruct the colour of the flower (see Table 1). Yet, photogrammetry is also subject to some
224 limitations (Table 1). Most obviously, flower models can be reconstructed for only externally visible parts of the
226 flower. Hidden structures, such as reproductive organs in some species, may remain hidden in particularly closed
228 corollas. Floral dissection might in some cases provide the means to characterise concealed structures in 3D using
photogrammetry, e.g., removal of the corolla, or simply cutting the sepals to reveal the base of the corolla, as we did
in the application example using Gesneriaceae. In addition, concealed organs can be photographed and thus be visible
on the model texture, allowing them to be analysed. But if concealed organs are of main interest for a given study,
microCT is clearly the best option.

230 Some flower characteristics also likely complicate the 3D model reconstruction with photogrammetry. One of
these is the often very thin surfaces of flowers. Missing surfaces or edges in the final 3D model often result from a
232 miscalculation of the position of sufficiently close outer and inner surfaces of an object to be modelled. Depth data
from sets of images may intersect, thus creating holes in the 3D mesh. A contrasting background and accurate masking
234 of flowers allow recovery of thin structures at the extremities of the models such as fringed petals or stamen filament
(e.g. see interactive flowers of *Rhytidophyllum vernicosum* and *Salvia nemorosa*). Shiny or translucent surfaces also
236 represented a challenge because the reflection of light or the features that are detected behind the translucent petals
are not fixed features on the surface, but are still captured in images. This issue can be solved by using a softer
238 light during the photography step. The presence of dense hairs on the flower also complicates model reconstruction
because of the difficulty of adequately removing the background on photographs and because the resulting model
240 is often rugged, although it can generally be corrected by smoothing the 3D surface. Finally, radially symmetrical
or spherical objects with no clear visual landmarks are typically difficult to reconstruct using photogrammetry (Ijiri
242 et al., 2018), such as some actinomorphic flowers. A straightforward solution is placing a few visually distinct markers
on such flowers (i.e. coloured dots) to add artificial distinct features to help the software to align the photographs.

244 Overall, ultra-close-range photogrammetry is an useful alternative to microCT scanning and could be valuable for
studies interested in the non-occluded parts of a flower and its colour. One interesting avenue is to combine CT-based
246 and image-based approaches to get the advantages of both approaches, as demonstrated by Ijiri et al. (2018).

Characteristics	Approaches	
	Photogrammetry	microCT scan
3D reconstruction of occluded areas and internal structures	No	Yes
Model colour and texture	Yes	No
Portability	Yes	No, but flowers can be fixed on site
Adaptable to any type of flower	Yes, but very soft and hairy flowers and those with few clear visual landmarks are more difficult to reconstruct	yes
Deformation of structures	no	slight
Cost	from \$2000	\$200,000 to \$1,000,000
Time requirements per flower	Setup and photography: 30min Colour calibration: 10min Reconstruction: 30min to 3h	Staining: typically > 14 days Scanning: 1h Segmentation: 30min to 5h

Table 1: Summary of the capabilities of both the microCT scan and photogrammetry approaches. Details on costs associated with photogrammetry are available in the Supporting Information Table S1.

5.2 Perspectives for floral morphology studies

248 5.2.1 Studying high-dimensional floral shape evolution

One obvious application of 3D flower models obtained by photogrammetry is to study floral shape. Different methods exist for characterising biological shapes in 3D. The most popular type of methods are geometric morphometrics that are based on the positioning of landmarks (homologous points) and semi-landmarks (points that are positioned relative to others, along curves or surfaces). Landmark-free methods have also been developed and could be useful for smooth or featureless 3D surfaces for which landmark placement is not appropriate (Pomidor et al., 2016). Our worked example on Gesneriaceae showed how photogrammetry can be used to study the three-dimensional morphology of flowers. The accurate three-dimensional reconstruction of flowers combined with landmark-based geometric morphometrics allowed better discrimination and understanding of the 3D structure of the distinct pollination syndromes (Fig.4) compared to what can be obtained using 2D shape information from flowers in profile view (Joly et al., 2018).

258 5.2.2 Studying flower colour in 3D

One obvious advantage of photogrammetry over other approaches is to provide a very accurate reconstruction of flower colour in 3D. This opens many study opportunities as flower pigmentation is a major display signal for animal-pollinated plants. The complexity of floral colouration, including nectar guides, help pollinators limit the time they spend locating rewards, thus improving their foraging efficiency (Leonard and Papaj, 2011). Moreover, both biotic factors, such as pollinator abundance and the colour of co-occurring plants in the community, and abiotic factors such as solar radiation and low precipitation, can influence the colour perception and patterns of flowers (Dalrymple et al., 2020).

266 We showed that photogrammetry is a valuable tool to recover calibrated colour information from the entire 3D surface of flowers. 3D textures generated directly from calibrated high-quality photos in colour analyses can account 268 for the totality of variation in flower pigmentation, avoiding biases caused by overlooked concealed surfaces or the

distorted importance given certain regions of the flower (surfaces perpendicular to the camera compared to those
270 that are more parallel) when using only a few 2D images in such analyses. Moreover, the presence of colour on 3D
models could facilitate the distinction of structures that vary in colour but not so much in shape. For example,
272 some species of Merianieae have stamen appendages that are distinguished from anthers primarily by their colour.
Retaining colour on 3D models could thus help the positioning of these structures to test alternative hypotheses of
274 floral modularity (Dellinger et al., 2019). The use of 3D models of flowers that retain colour information would greatly
assist in distinguishing organs that differ in function and colour, but are difficult to distinguish based on shape.

276 Photography is a convenient way to collect morphological and reflectance data (colour) from specimens, and to
facilitate research in ecology and evolution. However, the lack of tools to make objective colour measurements and
278 the fact that cameras generally used in scientific studies produce uncalibrated photographs unreliable for quantitative
colour measurements (Troscianko and Stevens, 2015). For this reason, a particular attention needs to be given to
280 photo calibration and linearisation.

In addition, photography is not restricted to the visible spectrum (wavelength from 400 to 700 nm). Light can be
282 detected by camera sensors in the UV range (320 to 400 nm) and IR (also called "heat radiation") or near-infrared
(NIR) range (over 700 nm to about 1 mm), making it possible to incorporate these components of the light spectrum
284 in 3D models. This could be important to understand patterns of reflectance evolution as most insect pollinators
possess UV receptors (Chittka et al., 2001; Schiestl and Johnson, 2013), and self-heating flowers or inflorescences
286 (Thien et al., 2000) as a reward or a means of enhancing the production and dissemination of floral scents (Seymour
et al., 2003). Furthermore, images could be converted to correspond to different animal visual system sensitivities
288 (cone-catch values) (Troscianko and Stevens, 2015).

5.2.3 Experimental studies

290 Advancements in 3D printing technology enable printing relatively small and intricate 3D models as well as remarkably
detailed colour patterns, directly (using coloured filaments) or indirectly (by applying colour on models). In addition
292 to colour, soft and flexible resins can be used thinly to resemble the soft tissues of flowers (see Supporting Information
Fig. S8 for an example of a colourless soft 3D printed artificial flower of a 3D model derived from photogrammetry).
294 These methods should help expand the scope of experimental studies designed to test hypotheses about pollinator
behaviour and flower shape, size and colour. As an example, printed artificial flowers and chimeric flowers made of
296 artificial and natural flower parts were used to decouple and test the relative contributions of olfactory and visual
signals to attract pollinators in a mimetic orchid *Dracula lafleurii* by Policha et al. (2016).

298 5.3 Natural history collections 3.0

Digitisation and archiving of information of material from natural history collections have revolutionised their current
300 use. 3D modelling of natural history collections would further advance their value, accessibility and use. Such efforts
are ongoing in entomological and ornithological collections using photogrammetry (Ströbel et al., 2018; Medina et al.,
302 2020). Unlike zoological specimens, which generally retain their 3D shapes in collections, plant specimens are usually
kept pressed in herbaria, thus losing most of their natural shape. Although morphological data can be extracted from
304 herbarium specimens (e.g., Bilbao et al., 2021), morphological correlations between flower parts are generally lost.
One strength of photogrammetry is that 2D data sets can be collected in the field to reconstruct 3D morphological
306 features lost in herbarium specimens and can be subsequently linked to them in similar ways as other sources of
information, such as genetic data or plants parts preserved separately from the specimens. Sharing such 3D models
308 would significantly improve the quality of phenomic data obtainable from herbaria (Ströbel et al., 2018; Medina et al.,
2020) or complement and extend the information on plant traits (morphological, anatomical, functional, biochemical,
310 phenological, and physiological) that is being centralised in global databases such as TRY (Kattge et al., 2011, 2020)
and PROTEUS (Sauquet, 2019). Photogrammetry could also be extended to living collections, such as botanical
312 gardens, thus improving access to such collections by providing access to virtual plants all year round and from

anywhere in the world, creating new opportunities for scientific studies and outreach (Maschner et al., 2013). Open
314 access databases dedicated to natural history, cultural heritage, and scientific collections are already available for such
applications (Boyer et al., 2016).

316 **6 Conclusions**

Due to its simplicity and efficacy, photogrammetry has the potential to inspire new ways to quantify flower shape and
318 colour and explore questions and collaborations in investigations of flowering plant evolution. Combined with genomic
data, phenomic information obtained from 3D models using photogrammetry will open new areas of study of floral
320 evolution. By combining practicality, reasonable costs, portability, and user friendly applications, photogrammetry
has the potential to revolutionise studies of floral evolution and ecology.

322 **7 Data availability**

The 3D model data are openly available in Morphosource at <https://www.morphosource.org/>, reference ID: 000369440.

324 **8 Acknowledgments**

We thank Diana Constanza Díaz for reconstructing the 3D model of *Paliavana prasinata* used in this study, and
326 for testing the user-friendliness of our detailed photogrammetry protocol. We thank Viraj Alimchandani for helping
3D-printing the 3D model of a flower belonging to *Gesneria cornuta*. We thank Anthony Smith for the handling and
328 preparation for CT-scans, and Hoai-Nam Bui for the CT-scanning and and 3D model reconstruction of flowers derived
from CT-scans. We also thank Janique Perreault and her team at the Montreal Botanical Garden for maintaining the
330 Gesneriaceae collection. Finally, we acknowledge the constructive comments of Agnes Dellinger and an anonymous
reviewer on a previous version of this paper. The Natural Sciences and Engineering Research Council of Canada
332 supported this research with Discovery Grants to SJ (05027-2018) and DS (74127-2017).

9 Conflict of interests

334 The authors have no conflicts of interest to declare.

10 Authors contributions

336 DS, ML and SJ designed the research. ML, JB and SJ acquired the data. ML and SJ analysed the data. ML wrote
the manuscript. ML, SJ, DS and JB edited and revised the manuscript. SJ and DS acquired funding.

338 **References**

- Agisoft LLC (2021). Agisoft metashape user manual: Professional edition, version 1.7.
- 340 Artuso, S., Gamisch, A., Staedler, Y. M., Schönenberger, J., and Comes, H. P. (2021). Evidence for selectively
constrained 3d flower shape evolution in a late miocene clade of malagasy bulbophyllum orchids. *New Phytologist*,
342 232(2):853–867.
- Artuso, S., Gamisch, A., Staedler, Y. M., Schönenberger, J., and Comes, H. P. (2022). Evidence for an evo-devo-
344 derived hypothesis on 3d flower shape modularity in a tropical orchid clade. *Evolution; International Journal of
Organic Evolution*.

- 346 Bilbao, G., Bruneau, A., and Joly, S. (2021). Judge it by its shape: a pollinator-blind approach reveals convergence
in petal shape and infers pollination modes in the genus erythrina. *American journal of botany*, 108(9):1716–1730.
- 348 Boyer, D. M., Gunnell, G. F., Kaufman, S., and McGeary, T. M. (2016). Morphosource: archiving and sharing 3-d
digital specimen data. *The Paleontological Society Papers*, 22:157–181.
- 350 Chittka, L., Spaethe, J., Schmidt, A., and Hickelsberger, A. (2001). *Adaptation, constraint, and chance in the evolution
of flower color and pollinator color vision*, page 106–126. Cambridge University Press.
- 352 Christiansen, F., Sironi, M., Moore, M. J., Di Martino, M., Ricciardi, M., Warick, H. A., Irschick, D. J., Gutierrez,
R., and Uhart, M. M. (2019). Estimating body mass of free-living whales using aerial photogrammetry and 3d
354 volumetrics. *Methods in Ecology and Evolution*, 10(12):2034–2044.
- Cunliffe, A. M., Brazier, R. E., and Anderson, K. (2016). Ultra-fine grain landscape-scale quantification of dryland
356 vegetation structure with drone-acquired structure-from-motion photogrammetry. *Remote Sensing of Environment*,
183:129–143.
- 358 Dalrymple, R. L., Kemp, D. J., Flores-Moreno, H., Laffan, S. W., White, T. E., Hemmings, F. A., and Moles, A. T.
(2020). Macroecological patterns in flower colour are shaped by both biotic and abiotic factors. *New Phytologist*,
360 228(6):1972–1985.
- Davies, T. G., Rahman, I. A., Lautenschlager, S., Cunningham, J. A., Asher, R. J., Barrett, P. M., Bates, K. T.,
362 Bengtson, S., Benson, R. B., Boyer, D. M., et al. (2017). Open data and digital morphology. *Proceedings of the
Royal Society B: Biological Sciences*, 284(1852):20170194.
- 364 Dellinger, A. S., Artuso, S., Pamperl, S., Michelangeli, F. A., Penneys, D. S., Fernández-Fernández, D. M., Alvear,
M., Almeda, F., Scott Armbruster, W., Staedler, Y., and Schönenberger, J. (2019). Modularity increases rate of
366 floral evolution and adaptive success for functionally specialized pollination systems. *Communications Biology*,
2(1):1–11.
- 368 Evin, A., Souter, T., Hulme-Beaman, A., Ameen, C., Allen, R., Viacava, P., Larson, G., Cucchi, T., and Dobney, K.
(2016). The use of close-range photogrammetry in zooarchaeology: Creating accurate 3d models of wolf crania to
370 study dog domestication. *Journal of Archaeological Science: Reports*, 9:87–93.
- Faegri, K. and Van Der Pijl, L. (1979). Principles of pollination ecology. *New York: Pergamon Press*, 64.
- 372 Fenster, C. B., Armbruster, W. S., Wilson, P., Dudash, M. R., and Thomson, J. D. (2004). Pollination syndromes
and floral specialization. *Annual Reviews of Ecology Evolution and Systematic*, 35:375–403.
- 374 Florey, C. L. and Moore, P. A. (2019). Analysis and description of burrow structure in four species of freshwater
crayfishes (decapoda: Astacoidea: Cambaridae) using photogrammetry to recreate casts as 3d models. *The Journal
376 of Crustacean Biology*, 39(6):711–719.
- Gamisch, A., Staedler, Y. M., Schönenberger, J., Fischer, G. A., and Comes, H. P. (2013). Histological and micro-ct
378 evidence of stigmatic rostellum receptivity promoting auto-pollination in the madagascan orchid bulbophyllum
bicoloratum. *PLoS One*, 8(8):e72688.
- Giacomini, G., Scaravelli, D., Herrel, A., Veneziano, A., Russo, D., Brown, R. P., and Meloro, C. (2019). 3d
photogrammetry of bat skulls: perspectives for macro-evolutionary analyses. *Evolutionary Biology*, 46(3):249–259.
- Hsu, H.-C., Chou, W.-C., and Kuo, Y.-F. (2020). 3d revelation of phenotypic variation, evolutionary allometry,
and ancestral states of corolla shape: a case study of clade corytholoma (subtribe ligeriinae, family gesneriaceae).
382 *GigaScience*, 9(1):1–16.

- Iglhaut, J., Cabo, C., Puliti, S., Piermattei, L., O'Connor, J., and Rosette, J. (2019). Structure from motion photogrammetry in forestry: A review. *Current Forestry Reports*, 5(3):155–168.
- Ijiri, T., Todo, H., Hirabayashi, A., Kohiyama, K., and Dobashi, Y. (2018). Digitization of natural objects with microct and photographs. *PloS one*, 13(4):e0195852.
- Joly, S., Lambert, F., Alexandre, H., Clavel, J., Léveillé-Bourret, E., and Clark, J. L. (2018). Greater pollination generalization is not associated with reduced constraints on corolla shape in Antillean plants. *Evolution*.
- Kattge, J., Bönisch, G., Díaz, S., Lavorel, S., Prentice, I. C., Leadley, P., Tautenhahn, S., Werner, G. D., Aakala, T., Abedi, M., et al. (2020). Try plant trait database—enhanced coverage and open access. *Global change biology*, 26(1):119–188.
- Kattge, J., Diaz, S., Lavorel, S., Prentice, I. C., Leadley, P., Bönisch, G., Garnier, E., Westoby, M., Reich, P. B., Wright, I. J., et al. (2011). Try—a global database of plant traits. *Global change biology*, 17(9):2905–2935.
- Katz, D. and Friess, M. (2014). 3d from standard digital photography of human crania—a preliminary assessment. *American Journal of Physical Anthropology*, 154(1):152–158.
- Leonard, A. S. and Papaj, D. R. (2011). ‘x’marks the spot: The possible benefits of nectar guides to bees and plants. *Functional Ecology*, 25(6):1293–1301.
- Linder, W. (2009). *Digital photogrammetry*, volume 1. Springer.
- Luhmann, T., Robson, S., Kyle, S., and Boehm, J. (2013). *Close-range photogrammetry and 3D imaging*. Walter de Gruyter.
- Maschner, H. D., Schou, C. D., and Holmes, J. (2013). Virtualization and the democratization of science: 3d technologies revolutionize museum research and access. In *2013 Digital Heritage International Congress (DigitalHeritage)*, volume 2, pages 265–271. IEEE.
- Mathys, A., Brecko, J., and Semal, P. (2013). Comparing 3d digitizing technologies: what are the differences? In *2013 Digital Heritage International Congress (DigitalHeritage)*, volume 1, pages 201–204. IEEE.
- Medina, J. J., Maley, J. M., Sannapareddy, S., Medina, N. N., Gilman, C. M., and McCormack, J. E. (2020). A rapid and cost-effective pipeline for digitization of museum specimens with 3d photogrammetry. *Plos one*, 15(8):e0236417.
- Policha, T., Davis, A., Barnadas, M., Dentinger, B. T. M., Raguso, R. A., and Roy, B. A. (2016). Disentangling visual and olfactory signals in mushroom-mimicking Dracula orchids using realistic three-dimensional printed flowers. *New Phytologist*, pages n/a–n/a.
- Pomidor, B. J., Makedonska, J., and Slice, D. E. (2016). A landmark-free method for three-dimensional shape analysis. *PloS one*, 11(3):e0150368.
- Reich, D., Berger, A., von Balthazar, M., Chartier, M., Sherafati, M., Schönenberger, J., Manafzadeh, S., and Staedler, Y. M. (2020). Modularity and evolution of flower shape: the role of function, development, and spandrels in erica. *New Phytologist*, 226(1):267–280.
- Rohlf, F. J. and Marcus, L. F. (1993). A revolution morphometrics. *Trends in ecology & evolution*, 8(4):129–132.
- Sauquet, H. (2019). Proteus: A database for recording morphological data and fossil calibrations.
- Schiestl, F. P. and Johnson, S. D. (2013). Pollinator-mediated evolution of floral signals. *Trends in ecology & evolution*, 28(5):307–315.

- 422 Seymour, R. S., White, C. R., and Gibernau, M. (2003). Heat reward for insect pollinators. *Nature*, 426(6964):243–244.
- 424 Staedler, Y. M., Masson, D., and Schönenberger, J. (2013). Plant tissues in 3d via x-ray tomography: simple contrasting methods allow high resolution imaging. *PLoS one*, 8(9):e75295.
- 426 Ströbel, B., Schmelzle, S., Blüthgen, N., and Heethoff, M. (2018). An automated device for the digitization and 3d modelling of insects, combining extended-depth-of-field and all-side multi-view imaging. *ZooKeys*, (759):1–27.
- 428 Stuppy, W. H., Maisano, J. A., Colbert, M. W., Rudall, P. J., and Rowe, T. B. (2003). Three-dimensional analysis of plant structure using high-resolution x-ray computed tomography. *Trends in plant science*, 8(1):2–6.
- 430 Thien, L. B., Azuma, H., and Kawano, S. (2000). New perspectives on the pollination biology of basal angiosperms. *International Journal of Plant Sciences*, 161(S6):S225–S235.
- 432 Timerman, D. and Barrett, S. C. (2019). Comparative analysis of pollen release biomechanics in thalictrum: implications for evolutionary transitions between animal and wind pollination. *New Phytologist*, 224(3):1121–1132.
- 434 Troscianko, J. and Stevens, M. (2015). Image calibration and analysis toolbox—a free software suite for objectively measuring reflectance, colour and pattern. *Methods in Ecology and Evolution*, 6(11):1320–1331.
- 436 van der Niet, T., Zollikofer, C. P., de León, M. S. P., Johnson, S. D., and Linder, H. P. (2010). Three-dimensional geometric morphometrics for studying floral shape variation. *Trends in plant science*, 15(8):423–426.
- 438 Wang, C.-N., Hsu, H.-C., Wang, C.-C., Lee, T.-K., and Kuo, Y.-F. (2015). Quantifying floral shape variation in 3d using microcomputed tomography: a case study of a hybrid line between actinomorphic and zygomorphic flowers. *Frontiers in plant science*, 6:724.
- 440 Willmer, P. (2011). *Pollination and floral ecology*. Princeton University Press.

11 Supplementary information

- 442 **Table S1** Summary of the materials used to scan and reconstruct three-dimensional flower models and their approximate price in 2022. Alternative materials can be considered, and we give as an example the specific materials we used when relevant.
- 444 **Table S2** Summary of the camera and turn table settings used to scan flowers.
- 446 **Fig. S1** Three-dimensional models of flowers of *Gesneria acaulis* (75-2021) obtained from photogrammetry and CT scanning.
- 448 **Fig. S2** Three-dimensional models of flowers of *Rhytidophyllum exsertum* (112-1991) obtained from photogrammetry and CT scanning.
- 450 **Notes S1** Taxonomic groups and flower material
- 452 **Table S3** Species and collection numbers associated with the Botanical Garden of Montreal database of the specimens used to reconstruct 3D models of flowers. Each species is associated with a pollination syndrome. The bibliographic reference identifying the pollination syndromes of each species is also listed. Pollination syndromes that are not confirmed were inferred.
- 454 **Methods S1** 3D Geometric morphometrics.
- 456 **Fig. S3** Example of landmarks and semi-landmarks placement on the corolla of *Gesneria cuneifolia* and *Gesneria cornuta*.
- 458 **Table S4** Identification of the landmark and semi-landmarks used for curves and surfaces.
- 460 **Fig. S4** Morphospace of individual 3D floral shape variation along the second and third principal axes of the PCA
- Fig. S5** Mean floral shapes for three pollination syndromes
- Fig. S6** Principal component analysis of floral shapes of Gesneriaceae according to pollination syndromes and the

⁴⁶² method used to reconstruct the 3D floral shapes.

Methods S2 Phylogenetic analysis

⁴⁶⁴ **Methods S3** Flower colour variation analysis

Fig. S7 Colour distance matrix heatmap and dendrogram using Ward's distance.

⁴⁶⁶ **Fig. S8** Example of a 3D-printed flower of *Gesneria cornuta* in clear and soft resin.